

# Some Augmented Cathode Follower Circuits\*

J. ROSS MACDONALD†

**Summary**—Some direct-coupled augmented cathode-follower circuits are described suitable for power-tube grid drivers, coaxial cable drivers, high-input impedance isolation stages, active electronic filters, and frequency selective circuits. One of the circuits, using only 2½ double triodes, has an input-output voltage transfer ratio of 0.995 or greater with no phase reversal, can supply up to 100 ma of positive current, has a frequency response essentially flat from zero up into the megacycle-second range, can have an input capacitance approaching or equal to zero, exhibits an input resistance greater than 10<sup>11</sup> ohms for input swings of ±100 volts or more using ordinary unselected receiving tubes, has an output resistance of 3 ohms, will handle a dynamic range of 630 volts peak-to-peak, and shows less than one part in a million total harmonic distortion at 20-volts rms output and only two parts in 10<sup>6</sup> distortion at 100 volts rms output.

## INTRODUCTION

THE CIRCUITS which are discussed in this paper have very high input impedance, low output impedance, wide dynamic range, extremely low distortion, frequency response from zero to the megacycle/second range, and input-output transfer ratios very close to or exceeding unity with no phase reversal. They are suitable for many applications. They may be used as grid drivers of high-power output tubes and will supply 100 ma or more of positive grid current in such service. They are suitable as isolation stages or buffers, particularly where their extremely high-input impedance characteristics are desirable. Their lack of phase reversal together with transfer ratios equal to or exceeding unity and their vanishingly small distortion as well as wide dynamic range makes them particularly useful in active electronic filters and frequency selective amplifiers.

The circuits to be discussed occupy a somewhat intermediate position between ordinary cathode followers and operational amplifiers. An unmodified cathode follower has relatively high input impedance, an unloaded ac input-output transfer ratio generally less than 0.98, an appreciable input-output dc offset, a fairly wide dynamic range, an output impedance of several hundred ohms, and frequency response up to the megacycle/second region. On the other hand, an operational amplifier generally has ac and dc voltage amplification very close to or greater than unity, very low nonlinear distortion, an output impedance of a few ohms or less, and a frequency response ranging from a few to a few hundred kilocycles.

## THE PACFD

Previously, a parallel augmented cathode-follower driver (PACFD) has been discussed [1] and incorporated as an output-tube grid driver in a high-quality audio

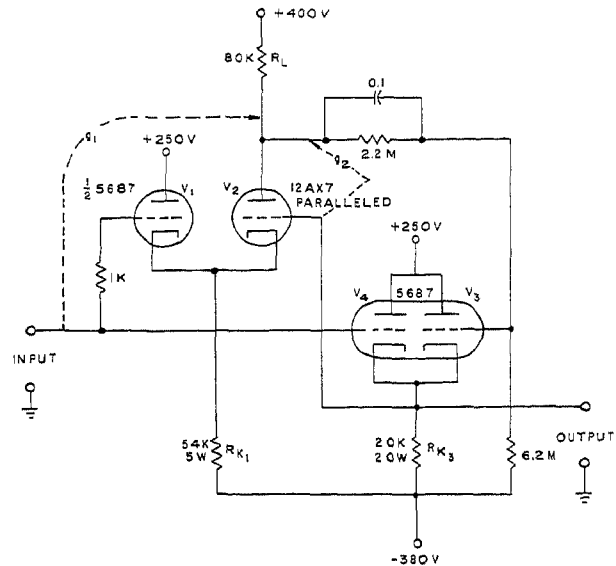


Fig. 1—The parallel augmented cathode-follower driver (pacfd) circuit.

TABLE I

Circuit Designation	Input-Output Transfer Ratio, $G$	Output Resistance, $r_o$
CF	$\mu / [\mu' + r_p / R_K]$	$r_p / [\mu' + r_p / R_K]$
PACFD	$\frac{\mu_3 g_1 + \mu_4 r_{p_3} / r_{p_4}}{[\mu_3 g_2 + \mu_3' + \mu_4 r_{p_3} / r_{p_4} + r_{p_3} / R_{K_3}]}$	$\frac{r_{p_3}}{[\mu_3 g_2 + \mu_3' + \mu_4 r_{p_3} / r_{p_4} + r_{p_3} / R_{K_3}]}$
ACF-1	$\frac{\mu_3 g_1}{\mu_3 g_2 + \mu_3' + r_{p_3} / R_{K_3}}$	$\frac{r_{p_3}}{\mu_3 g_2 + \mu_3' + r_{p_3} / R_{K_3}}$
ACF-2	See text	See text

amplifier [2]. This circuit, shown in Fig. 1, is more complex than an ordinary cathode follower, has an output resistance of 5.6 ohms, an input-output transfer ratio of 0.986, and can supply up to 200 ma of positive driving current without excessive distortion. Table I presents expressions for the mid-frequency input-output transfer ratio,  $G$ , and output resistance,  $r_o$ , of several of the circuits with which we shall be concerned. The arithmetic amplifications  $g_1$  and  $g_2$  which appear in some of these formulas are [3]

$$g_1 = \left[ \frac{\mu_1}{\mu_1' + r_{p_1} / R_{K_1}} \right]$$

$$\cdot \left[ \frac{\mu_2'}{1 + r_{p_2} / R_L + (\mu_2' r_{o_1} / R_L) / (\mu_1' + r_{p_1} / R_{K_1})} \right], \quad (1)$$

$$g_2 = \mu_2 [1 + r_{p_2} / R_L + (\mu_2' r_{p_1} / R_L) / (\mu_1' + r_{p_1} / R_{K_1})]^{-1}, \quad (2)$$

\* Manuscript received by the PGA, January 9, 1957.  
 † Texas Instruments, Inc., Dallas 9, Tex.

where  $\mu' = \mu + 1$ , the subscripts refer to tubes  $V_1$  and  $V_2$ , and loading of  $V_3$  on  $V_2$  is neglected—usually a good approximation. Note that the algebraic amplification corresponding to  $g_2$  is negative.

### THE ACF-1

The PACFD circuit of Fig. 1 is not an optimum design in terms of number of tube halves employed and minimization of dc offset. It can be simplified and improved, as in Fig. 2, by eliminating the direct signal path through  $V_4$  and by either omitting this tube half or connecting it in parallel with  $V_3$ . The resulting circuit with the two sections of a 5687 tube in parallel will supply as much positive driving current as the PACFD and can be adjusted (e.g., by varying  $R_L$ ,  $R_{K_1}$ , etc.) so that there is no dc offset for a given quiescent dc input operating level. We shall designate the augmented cathode-follower circuit of Fig. 2, using only a single output tube half for  $V_3$  by the acronym acf-1. As Table I shows, its transfer ratio and output resistance are not much different from that of the PACFD; thus, its output resistance is still of the order of 5 to 6 ohms for the values shown in Fig. 2. The acf-1 is not particularly new; a similar arrangement has been used for some time in connection with frequency-selective amplifiers<sup>1</sup> where the frequency-discriminating circuit is inserted in the feedback line  $a$  of Fig. 2.

The acf-1 has a transfer ratio  $G$  slightly less than unity when connected as in Fig. 2. It may be readily modified, however, to have a  $G$  of exactly unity or a greater amplification almost as large as  $g_1$ . Increased amplification is produced most simply by tapping the feedback line  $a$  down on the output cathode resistor  $R_{K_3}$  as shown in Fig. 3. The resulting negative feedback reduction is equivalent to a decrease in  $g_2$  with  $g_1$  remaining constant. As Table I shows, such a decrease increases both  $G$  and the output resistance  $r_0$ . A useful feature of the circuit is that amplifications of the order of 1 to 10 are still achieved with quite low output impedance and with no phase inversion. These features make the acf-1 well suited for the active element in active RC filters [3, 5, 6]. Note, however, that when line  $a$  is tapped very far down on  $R_{K_3}$ , the voltage divider between  $V_2$  and  $V_3$  may have to be adjusted, and the quiescent dc output level begins to exceed that of the input appreciably. This result is often of no consequence; it need not exist, of course, with ac coupling between  $V_2$  and  $V_3$ .

The acf-1 circuit of Fig. 3 was designed specifically for an active filter [6] where it was important that the transfer ratio be essentially independent of supply voltages, that amplifications slightly greater than unity be achieved, and that the output impedance be low. The measured  $r_0$  for minimum  $G$  was 4.75 ohms at audio frequencies and 5.6 ohms at 0.5 mc. With a 12AT7 in place of the 12BZ7,  $r_0$  increased to 7.75 ohms at low

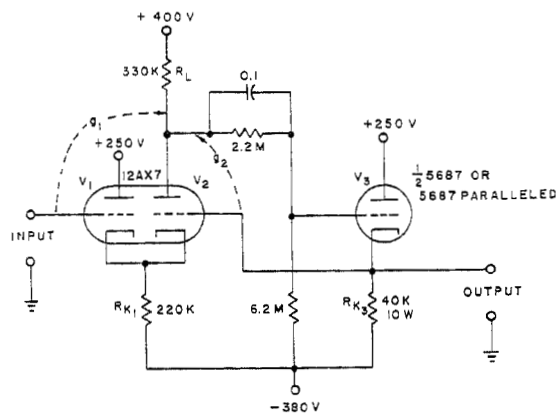


Fig. 2—The augmented cathode-follower number 1 circuit (acf-1).

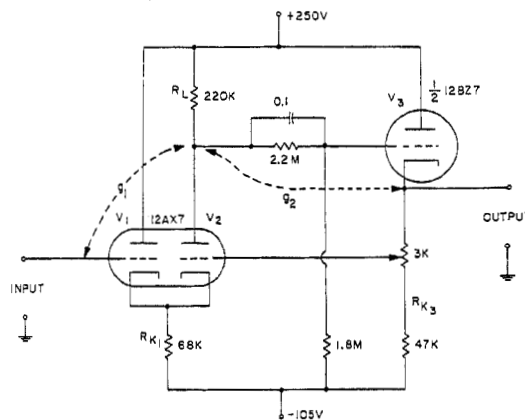


Fig. 3—The acf-1 circuit with voltage amplification control.

frequencies. The differential-signal transfer ratio  $G$  could be varied with the potentiometer shown between 0.97 and 1.07, and it varied by less than 0.1 per cent when the dc supply voltages were varied by  $\pm 10$  per cent.

### THE ACF-2

#### The Circuit

The acf circuits of Figs. 2 and 3 may still be considerably improved, although as they stand they are suitable for a wide variety of applications. Although their dynamic range is relatively large, it is limited by the quiescent voltage which may be applied to the tubes without exceeding their ratings and by the magnitude of the negative supply voltage. In addition, the main feedback loop is not effective in reducing nonlinear distortion generated in the input cathode follower  $V_1$ , although, being a cathode follower, its internal feedback helps keep such distortion low. Nevertheless, no matter how much the main loop feedback may reduce distortion in the rest of the circuit, the final limiting distortion will be that of  $V_1$ .

A first step is further distortion reduction, and further increase of the dynamic range is, therefore, the improvement of these quantities for  $V_1$ . First, we may replace  $R_{K_1}$  by a constant-current triode,<sup>2</sup> which has

<sup>1</sup> See Valley and Wallman [3], pp. 384-408.

<sup>2</sup> See Valley and Wallman [3], p. 432.

the effect of greatly increasing  $R_{K1}$  and of improving the dynamic range, particularly for large negative signals. Next, to reduce distortion further and to extend the dynamic range for positive signals without exceeding the quiescent 300-volt plate-voltage rating of these tubes, we may employ plate driving of  $V_1$  as shown in Fig. 4. We shall designate this circuit as the acf-2. Note that in order to extend the full amount of feedback down to zero frequency, two avalanche-breakdown silicon diodes are used for part of the divider between  $V_2$  and  $V_3$ . In their breakdown region, these diodes have very low ac or differential resistance, but a dc voltage drop nearly independent of current. Each diode in Fig. 4 is selected to have a drop of about 100 volts.

In addition to the constant-current tube  $V_5$ , the circuit of Fig. 4 differs from that of Figs. 2 and 3 by the presence of the cathode follower  $V_4$  which drives the plates of  $V_1$  and  $V_3$  with a signal very nearly equal to that at the input. Thus, for example, when the level at the input is increased by 100 volts, the plate and cathode of  $V_1$  both rise by nearly the same amount, as do the grid, cathode, and plate of both  $V_2$  and  $V_3$ . It is therefore evident that as long as none of the tubes are saturated or cut off, the effective dynamic operating points of  $V_1$ ,  $V_2$ , and  $V_3$  will be virtually independent of signal. Such independence means, in turn, that these tubes cannot generate appreciable distortion. Since there is a signal path through  $V_1$ ,  $V_2$ , and  $V_3$  from the input to the output, the output will be a virtually undistorted replica of the input. Furthermore, it is clear that although all the dc levels can be arranged so that no quiescent plate voltage exceeds 300 volts, the instantaneous plate voltage of  $V_1$ ,  $V_2$ , and  $V_3$  can increase, because of a positive input signal, until  $V_4$  is saturated. This behavior allows a very wide, undistorted dynamic range to be obtained without exceeding tube ratings. Note that the acf-2 can be constructed using only  $2\frac{1}{2}$  double triodes.

*Circuit Operation and Transfer Ratios*

Below are given some of the algebraic results of an approximate analysis of the mid-frequency equivalent circuit of Fig. 4 which shows that  $e_2$ ,  $e_3$ , and  $e_4$ , and  $e_K$  will all follow the input  $e_1$  closely. However, these results can be described in words as follows. The input

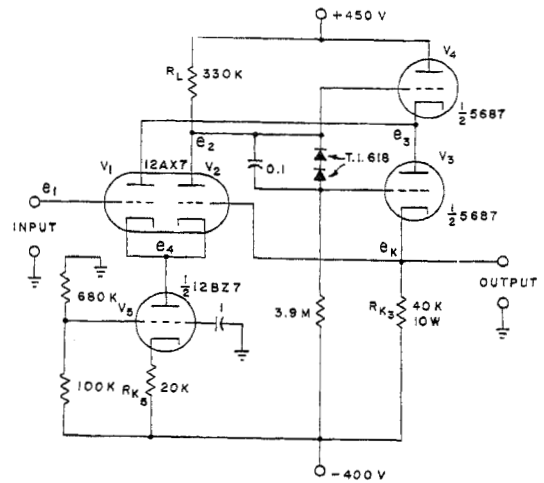


Fig. 4—The acf-2 circuit.

to  $e_1$ ,  $e_4$  will also almost equal  $e_1$ . Finally, the negative feedback between  $V_3$  and  $V_2$  will act in such sense that  $e_2$ , which equals  $e_4$  plus the amplified difference between  $e_4$  and  $e_K$ , will, in turn, be nearly equal to  $e_1$ . Because of the cathode follower action of  $V_3$ ,  $e_K$  must be smaller than  $e_2$ ;  $e_2$  will thus be slightly greater than  $e_4$  and may even exceed  $e_1$ . Note that driving the plate of  $V_3$  with the signal  $e_3$ , which is almost as large as  $e_2$ , makes  $e_K$  closer to  $e_2$  than would be the case if the plate of  $V_3$  were not so driven. If there were no loss between  $e_2$  and  $e_K$ , it would be easy to show that  $e_2$  and  $e_K$  would also equal  $e_4$ .

Although algebraic expressions for the various transfer ratios which may be defined for Fig. 4, have been worked out taking into account the loading of  $V_3$  and  $V_4$  on  $V_2$  and that of  $V_1$  on  $V_4$ , the results are exceptionally complicated and will not be given. Even when such loading is neglected, algebraic expressions for the transfer ratios are still long. We shall give those for  $G_2 = e_2/e_1$  and  $G = e_K/e_1$ , because of the light they throw on the distortion of the circuit. The main error occasioned by neglecting loading comes from omitting the effect of the plate current of  $V_1$  on the cathode current of  $V_4$ . Since the former will generally be at least ten times smaller than the latter for the circuit of Fig. 4, the error resulting from its neglect will be small.

We have the following approximate results

$$G_2 \cong \frac{\mu_1 \mu_2'}{\mu_1' \mu_2 M - \mu_2' N + \mu_1' \left(1 + \frac{r_{p2}}{R_L}\right) + \mu_2 \left(M \frac{r_{p1}}{R_{K1}} + \frac{r_{p1}}{R_L}\right) + \frac{r_{p1}}{R_L} \left(1 + \frac{R_L}{R_{K1}} + \frac{r_{p2}}{R_{K1}}\right)}, \tag{3}$$

$$G \cong MG_2, \tag{4}$$

signal to  $V_3$  will be essentially  $e_2$ , since no appreciable loss of signal occurs across the diode-capacitor combination. Further  $e_3$  will be nearly equal to  $e_2$ , since  $V_4$  is a cathode follower. Thus,  $e_K$  will also be nearly equal to  $e_2$ . Since  $e_1$ ,  $e_K$ , and  $e_3$  are all equal to or almost equal

where

$$M = \frac{\mu_3' \mu_4 + \mu_3}{\mu_3' \mu_4' + \mu_4' r_{p3} / R_{K3} + r_{p4} / R_{K3}}, \tag{5}$$

and

$$N = \frac{\mu_3' \mu_4 + \mu_4 r_{p3} / R_{K_3} - \mu_3 r_{p4} / R_{K_3}}{\mu_3' \mu_4' + \mu_4' r_{p3} / R_{K_3} + r_{p4} / R_{K_3}} \quad (6)$$

For simplicity, we have written the effective resistance of the constant current tube,  $r_{p3} + (\mu_3 + 1)R_{K_3}$  as  $R_{K_3}$ . For the circuit of Fig. 4,  $R_{K_3}$  is of the order of 2 megohms. The quantities  $M$  and  $N$  are less than unity. Eq. (3) shows that  $G_2$  may exceed unity; even so,  $G$  will be slightly less than unity. Note that the parameters of  $V_4$  enter the expression for  $G$  only through  $M$  and  $N$ . Further, for Fig. 4, these quantities may be approximated quite closely by

$$M \simeq \left[ \frac{\mu_3}{\mu_3' + r_{p3} / R_{K_3}} \right] \left[ \frac{1 + 2/\mu_4}{1 + 1/\mu_4} \right] \\ \cong \left( \frac{\mu_3}{1 + \mu_3} \right) \left( 1 + \frac{1}{\mu_4} \right), \quad (5a)$$

and

$$N \simeq \left[ \left\{ 1 + r_{p3} / (\mu_3' R_{K_3}) \right\} \left\{ 1 + 1/\mu_4 \right\} \right]^{-1} \\ \cong \left( 1 - \frac{1}{\mu_4} \right). \quad (6a)$$

Thus, to a good approximation only  $\mu_4$  enters  $M$  and  $N$  and then only as a second order term. Since  $\mu$  for a tube is relatively independent of operating point, the effect of the parameters of  $V_4$  on  $G$  is, therefore, exceedingly small and their changes arising from wide excursions of the input signal  $e_1$  will have a negligible effect on  $G$ . We may also note that (3)–(6) indicate that increasing the  $\mu$ 's and  $g_m$ 's of the various tubes will make  $G$  closer to unity.

The transfer ratio  $G$  may be made unity or greater by tapping down the feedback line in the manner of Fig. 3. Some of the other transfer ratios of the circuit may alternatively be made unity by inserting a resistor  $R_s$  in series with  $R_L$ , connecting the voltage divider for the grid of  $V_2$  at the junction of  $R_s$  and  $R_L$ , and connecting the grid of  $V_4$  to the junction of  $R_s$  and the plate of  $V_2$ . The method is illustrated in Fig. 9. Table II shows some experimental results for various transfer ratios measured on the acf-2 with  $e_1 = 10$  volts at  $10^8$  cps. The first row for  $R_s = 0$  shows that  $G_4 = e_4/e_1 = 0.9975$ ,  $G = 0.995$ , and that  $G_2$  is slightly greater than unity. These ratios are nearly independent of signal magnitude over a wide range and show that a 100-volt increase in the grid voltage  $e_1$  of  $V_1$  would lead to a 99.75-volt cathode rise and a 94.1-volt plate rise; as far as  $V_1$  is concerned the 100-volt input signal looks, therefore, like a 0.25-volt grid bias decrease and a cathode-to-plate voltage decrease of only 5.6 volts.

Table II shows that increasing  $R_s$  from zero to 21K causes  $G_3 = e_3/e_1$  to become unity, while an  $R_s$  of 82K makes  $G_4$  unity while causing  $G_2' (= e_2'/e_1)$  and  $G_3$  to be appreciably greater than unity. Here,  $e_2'$  is the signal at the plate of  $V_2$ , while  $e_2$  is that at the juncture of

TABLE II

$R_s$	$1-G_4$	$1-G_3$	$G_2'-1$	$1-G_2$	$1-G$
0	0.0025	0.059	0.0039	-0.0039	0.0050
21K	0.00178	~0	0.066	0.00068	0.0050
82K	~0	-0.182	0.260	0.0118	0.0050

$R_s$  and  $R_L$ . The quantities  $|1-G_i|$  given in Table II were determined by direct measurement of the difference between the two corresponding signals (e.g.,  $e_1 - e_4$ ) using a Ballantine type 310A ac voltmeter. The places in Table II marked ~0 are not shown as exactly zero, because they were limited to a minimum nonzero value by the exceedingly small nonlinear harmonic distortion components present in the output signal as compared to the input  $e_1$ , even when  $R_s$  was adjusted to make their fundamentals exactly equal.

Because of the feedback present in the acf-2, loading the output tends to increase  $G_2$  to compensate for such loading. For example, the connection of a 10K resistor across the output increases  $(G_2 - 1)$  to 0.024 and increases  $(1 - G)$  from 0.0050 and 0.0053 when measurements are made with  $e_1 = 10$  volts. The other transfer ratios do not change appreciably. Note that the acf-2 constructed with a type 5687 tube as in Fig. 4 can supply up to 100 milliamperes of positive current to a load. Its negative current is, of course, limited by the quiescent current in  $R_{K_3}$ . Increased positive current handling capacity could be achieved, if desired, by replacing the two sections of the 5687 tube by more powerful tubes such as the 6BX7-GT double triode.

#### Output Resistance, Frequency Response, and Capacitance Cancellation

Measurements of the acf-2 of Fig. 4 yielded an output resistance of 3 ohms and a frequency response into the megacycle/second range. At 0.5 mc,  $1 - G$  had only increased from its midfrequency value of 0.005 to 0.026. It may be noted that shielding the high-impedance portions of the circuit and driving the shield with the output signal  $e_K$  should allow a frequency response less than 3 db down to 10 mc or beyond. This cancellation of stray capacitance is effective when the input and output signals are very nearly equal as they are here; it may also be applied to cancel input capacitance such as that of a coaxial cable at the input [7]. Perfect cancellation is possible over a limited range of frequencies by adjusting  $G$  and/or  $G_3$  to the proper values.

#### Linear Operation Range

Fig. 5 shows curves of the dc linearity of the acf-2 with either two diodes in the voltage divider chain as shown in Fig. 4 or with only one such diode. Here we plot  $\Delta E = E_{in} - E_K$  vs  $E_{in}$ , where the capital letters denote dc voltages.  $\Delta E$  was measured directly with a Fluke Type 801 dc vtvm. The nonzero slopes of the central portions of these curves arise from the deviation of  $G$  from unity and are consistent with  $1 - G = 0.005$ . It

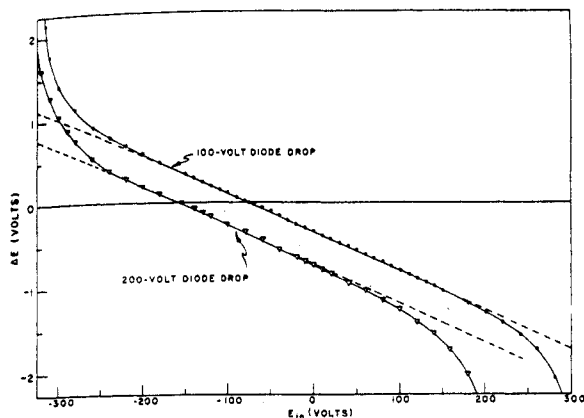


Fig. 5—Linearity curves for the acf-2.

is felt that the few visible deviations from the central straight lines are due to experimental error. For these regions, the device is so linear that deviations from linearity should not show up visually even on this magnified scale.

The deviations from linearity at the ends of the curves arise from the onset of positive or negative clipping. Even the extreme deviations shown at the ends of the curves represent only about one per cent departure from linearity. Note that with one diode,  $E_K = E_{in}$  for  $E_{in} = -75$  volts, while for both diodes, this point is reached at  $E_{in} = -155$  volts. This point may be varied and brought to  $E_{in} = 0$ , if desired, by changes in the values of  $R_{K_5}$  and/or  $R_L$ . Under these conditions, there would be no dc offset at  $E_{in} = 0$  and offset at any other value of  $E_{in}$  would be produced just by the slight departure of  $G$  from unity. Experimentally, this condition may be achieved by making  $R_{K_5} = 27K$  for the one-diode circuit, and  $39.5K$  for the two-diode circuit. These values of  $R_{K_5}$  apply when  $E_{in}$  is derived from a low impedance source.<sup>3</sup> It is found that a decrease in  $R_{K_5}$  somewhat increases the maximum undistorted output swing. With the one-diode circuit, the maximum span is increased from the  $+290 - (-290) = 580$  volts obtained with  $R_{K_5} = 20K$  to  $+290 - (-340) = 630$  volts with  $R_{K_5} = 13K$ . This swing of 630 volts is further increased to  $+350 - (-325) = 675$  volts if the positive supply voltage is changed from  $+450$  to  $+510$  volts. These swings were found to correlate well with measurements of the maximum ac output signals possible with the circuit. For these measurements, the dc bias applied to the input was adjusted to place the quiescent operating point in the center of the linear operating region shown in Fig. 5. By this means, positive and negative clipping of the ac signal could be made to occur together. With  $R_{K_5} = 20K$ , the

<sup>3</sup> If the input-output dc voltage offset is made zero for a given input level and at the same time, the input-output voltage transfer ratio is made exactly unity, then the dc offset will remain zero for any input with the dynamic range of the circuit. By proper adjustment of  $R_L$ ,  $R_{K_5}$ , and the amount of the signal  $e_2$  eventually fed back to the right grid of  $V_2$ , it should be possible to achieve the above result. Even when functioning in this ideal fashion with unity gain and zero dc offset, the other advantageous characteristics of the circuit should remain unimpaired.

one diode circuit did not show clipping until  $e_K > 206$  volts rms, equivalent to 583 volts peak-to-peak.

#### Input Resistance

We have already mentioned how input capacitance at the input of the acf-2 may be cancelled. For many applications, it is desirable to have exceedingly high input resistance as well. When the grid of tube  $V_1$  of Fig. 4 is left floating completely free, the output level is found to be  $-65$  volts. This value is determined by the grid-cathode bias of  $V_1$  at which positive and negative grid currents cancel.<sup>4</sup> Since the output follows the input, we may infer that the input grid also floats at a level of about  $-65$  volts. For infinitesimal input signals applied around  $-65$  volts which do not appreciably alter the grid-cathode bias of  $V_1$ , the input resistance is essentially infinite, since the grid current is zero. However, in the present circuit, one must remember that the cathode potential of  $V_1$  follows its grid potential very closely; hence, we may expect that appreciable input signals may be applied before the  $V_1$  grid-cathode bias changes enough to lower the input resistance greatly.

We have measured the input resistance  $r_i$  in two different ways. First, it may be found from measurements of the output level  $E_K$  when a given dc voltage is applied to the input directly and then through a large resistor. We have used resistors of  $10^9$ ,  $10^{10}$ ,  $10^{11}$ , and  $10^{12}$  ohms for this purpose. The input resistance may be calculated quite accurately from the inferred drop across the high input resistor. Secondly, it may be calculated from a capacitor discharge time. Here, a small high-quality capacitor is connected from the input to ground, charged to a given positive or negative voltage, and the source of charging voltage disconnected. The voltage level at the output is then observed as the capacitor discharges through  $r_i$ . The time,  $T$ , for the difference between the output level at the start of discharge and the final quiescent level to decrease to  $e^{-1}$  of its original value is then observed and  $r_i$  calculated from the result and the known value of capacitance. Mylar, mica, and air capacitors ranging from  $10^2$  to  $10^4$   $\mu\mu\text{f}$  have been used for such measurements. It has been found that the two methods yield comparable results.

We find for the circuit of Fig. 4 that  $r_i \approx 2 \times 10^9$  ohms when  $+100$  volts is applied to the input and  $4 \times 10^{10}$  ohms for  $-100$  volts. For the measurement of dc potentials and charges from a very high impedance source, it is desirable that the input grid float at or nearly at zero potential when left free. By adjusting  $R_{K_5}$ , we can readily change the floating point from  $E_K = -65$  volts with  $R_{K_5} = 20K$  to  $E_K = 0$  volts with  $R_{K_5} = 24K$ . Now, when  $E_{in}$  is  $+100$  or  $-100$  volts  $r_i$  is found to be  $1.6 \times 10^{10}$  and  $7 \times 10^{10}$  ohms, respectively. The results for smaller input swings are the same or higher. Comparable results are obtained when a single 100-volt-drop diode is used instead of the two of Fig. 4.

Although an input resistance of  $10^{10}$  ohms or greater

<sup>4</sup> See Valley and Wallman [3], p. 418.

is high enough for many applications, it was found that even higher values could be obtained in the following manner. The maintenance of an extremely high input impedance over a wide input voltage range depends, as we have noted, on the grid-cathode bias of  $V_1$  remaining at or nearly at its grid-current cancellation value independent of the actual input level. By making  $G_4=1$  by means of the series plate resistor  $R_s$  mentioned earlier, the ac and differential dc voltage transfer ratio from input to the cathode of  $V_1$  become unity and changes of input level should have no effect whatsoever on the grid-cathode potential of  $V_1$ . Such operation should, therefore, give increased input impedance over a wide range.

This idea was investigated and did indeed yield higher  $r_i$  values. It was here necessary to set  $R_s$  to some value greater than zero, then adjust  $R_{K_3}$  to make  $E_K=0$  with the input grid floating. The floating point is a fairly sensitive function of  $V_1$  heater current under these conditions, and it was found desirable to regulate the heater voltage for the entire circuit, to render  $E_K$  more stable with respect to time with the input floating. Increased stability was also achieved by replacing  $V_5$  with one-half of a 12AX7 instead of the 12BZ7 shown in Fig. 4. Such replacement did not appreciably affect  $r_i$ .

With  $R_s=50K$  and  $E_K=0$  with input floating,  $r_i$  was found to be  $2 \times 10^{11}$  and  $1 \times 10^{11}$  ohms for  $E_{in} = -100$  and  $+100$  volts, respectively. For  $R_s=75K$ ,  $r_i=5 \times 10^{11}$  ohms for swings of both  $-100$  and  $+100$  volts. The above values of  $R_s$  were insufficient to make  $G_4=1$ , but caused it to be closer to unity than with  $R_s=0$ . The floating point was quite stable under these conditions. It was found possible to further increase  $R_s$  to obtain  $r_i \approx 10^{12}$  ohms with fair stability of the floating point. However, when  $R_s$  was further increased to make  $G_4=1$ , the floating point was quite unstable,  $r_i$  was difficult to measure, and even unstable negative resistances could be observed. It is worth mentioning that the above results do not depend critically upon the choice of the 2AX7 used for  $V_1$  and  $V_2$ ; practically identical results were obtained with several different 12AX7's and 12AD7's. These results indicate that an input-output resistance transfer ratio exceeding  $10^{11}$  is obtainable with the acf-2. Since it responds linearly over a wide input signal range, the acf-2 would be very well suited for the input stages of a wide-range, extremely high input resistance ac-dc vacuum tube voltmeter. Using input capacitance cancellation, its effective input capacitance could also be held to a fraction of a micromicrofarad over a relatively wide frequency range.

#### Nonlinear Distortion

The exceptional linearity of the acf-2 suggested that it might be difficult or impractical to measure the exceedingly small amounts of nonlinear distortion to be expected for signals of medium amplitude. Such distortion has been measured, however, and the results are presented in Figs. 6 and 7. Fig. 6 shows how the total harmonic distortion of an ordinary cathode fol-

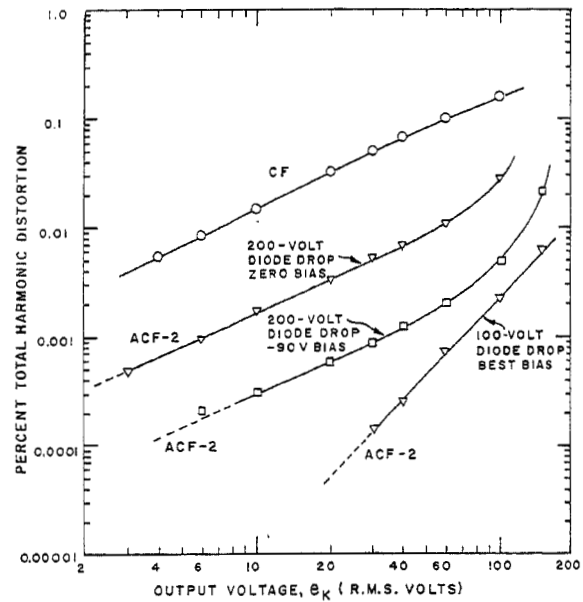


Fig. 6—Per cent total harmonic distortion of an ordinary cathode follower and the acf-2 vs output signal.

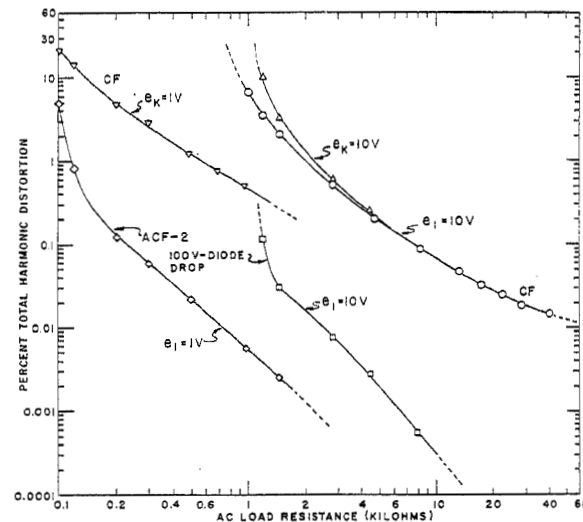


Fig. 7—Per cent total harmonic distortion of an ordinary cathode follower and the acf-2 vs total ac load for fixed signal magnitudes.

lower and of the acf-2 depend on output signal with no added load. The cathode follower used one-half of a 5687 tube with 250 volts applied to the plate and a cathode resistor of 40K connected to the  $-400$  volt supply. The frequency of the applied signals was  $10^3$  cps.

These low distortion measurements were made by the bridge method shown in the block diagram of Fig. 8. Since the input and output signals of the acf are essentially in phase at low frequencies and nearly equal, one can subtract a portion of the input equal in magnitude to the fundamental component of the output from the output and have left only the distortion components present in the output. Such subtraction occurs in the general radio bridge transformer of Fig. 8. This transformer has shielded input and output windings, and, by floating and grounding the shields as shown, the



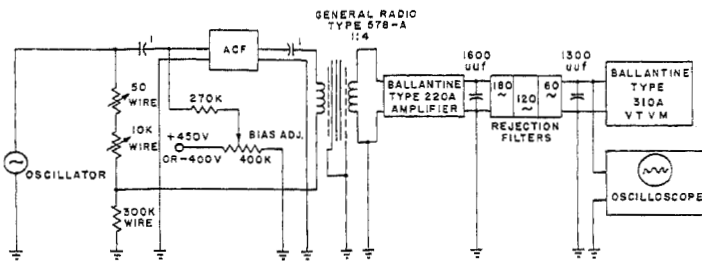


Fig. 8—Bridge circuit for measuring total harmonic distortion of a device having an input-output transfer ratio of unity or less.

large in-phase signal applied to both sides of the primary is essentially eliminated from the secondary. For perfect fundamental cancellation in the output, a capacitive balance (not shown) was often necessary, as well as the resistive balance produced by adjustment of the 50 ohm and 10K resistors. It may be noted that instead of balancing a reduced replica of the input against the output, it is possible to increase  $G$  to unity by the method of Fig. 3 and balance the output directly against the input. Both methods give equivalent results, although the circuit feedback is slightly reduced by the  $G=1$  adjustment.

Since the lowest distortion components measured were of the order of microvolts, it was necessary to reduce pickup and hum as much as possible. The Ballantine amplifier is battery operated, has amplifications of 10 or 100, and has low-internal noise generation. Residual hum components and high-frequency noise are sufficiently reduced by the shunting capacitors and parallel-T rejection filters shown. Before each use, the circuit of Fig. 8 was carefully calibrated as a function of frequency from the transformer input to the ac voltmeter. For the larger distortion components, the calibration could be checked and distortion measurements carried out by connecting the voltmeter or amplifier terminals directly to the bridge output normally connected to the transformer.

It was usually found using the above measuring apparatus and oscilloscope presentation that the distortion components were predominately second or third harmonics. Since we measure the rms value of the distortion and that of the fundamental plus harmonics, their quotient gives the total harmonic distortion,  $D_h$ , directly. Note in the log-log presentation of Fig. 6 that the slope of the cathode follower distortion and that of parts of the next two lower curves is very nearly unity. Such a linear dependence of  $D_h$  on fundamental signal magnitude is exactly what one would expect for pure second harmonic distortion, and it was verified by means of the oscilloscope that the distortion was, in fact, of just this character for these curves. On the other hand, the lowest curve is slightly steeper than the square-law dependence to be expected for pure third-order distortion. Here the bias was progressively adjusted from +30 to +90 volts to place the quiescent operating point of the acf-2 at the position on the dynamic trans-

fer characteristic that gave symmetric operation, thus greatly reducing even-order distortion generation. Note that the total harmonic distortion indicated by the lowest curve is less than one part in a million at 20 volts output and only two parts in a hundred thousand at 100 volts output.

Fig. 7 shows the dependence of the distortion of the various circuits on total loading (the parallel combination of added load and the 40K  $R_{K_3}$ ) for different fixed signal magnitudes. Measurements were carried out at  $10^3$  cps, and the added load was applied in series with a 15  $\mu$ f oil-filled capacitor. Since the acf-2 holds  $e_K$  essentially equal to  $e_1$  down to the point where negative clipping occurs, the acf-2 curves marked  $e_1=1$  or 10 volts are equivalent to similar curves with  $e_1$  replaced by  $e_K$ . The comparison between the cathode follower and the acf-2 is fairest when the  $e_K=\text{constant}$  cathode-follower curves are compared with the acf-2 curves, since for constant  $e_1$  loading reduces the output signal of the cathode follower quite appreciably so that negative peak clipping is not approached as rapidly as with  $e_K=\text{constant}$ . The rapid rises in the curves around loads of 1K and 100 ohms come from the approach of negative peak clipping, since the cathode current in both the circuits was approximately 10 ma. It will be noted that in both Figs. 6 and 7 the acf-2 has of the order of a hundred times less distortion than the simple cathode follower.

### THE ACF-3

Finally, in Fig. 9 we show a simplified acf circuit which we shall designate the acf-3 and which uses only two double triodes. This circuit has an output impedance of several hundred ohms, appreciably higher than that of the other augmented cathode followers. Its main advantages are that its ac and dc input-output transfer ratio can be made exactly unity (with the resulting exceedingly high input resistance already discussed in connection with the acf-2), and it can have essentially zero dc offset over a wide range. It is thus an impedance converter from very high-input impedance to moderately low-output impedance with unity transfer ratio and wide-frequency response extending from dc to tens of megacycles with driven shielding.

By adjusting the series resistor  $R_s$ ,  $e_2'$  may be increased to a value which makes the transfer ratio  $G_4=e_4/e_1$  or  $G_5=e_5/e_1$  exactly unity. The resistor  $R_0$  is then adjusted to make the dc drop across it exactly equal to the grid-cathode bias of  $V_1$ . Then the dc output will also be exactly equal to the input. Since  $V_3$  is a constant-current tube having very high differential resistance, the dc current through  $R_0$  will be held nearly constant and independent of the input signal magnitude or level. Further, since the transfer ratio  $G_4$  is unity for differential changes, the grid-cathode bias of  $V_1$  is also virtually independent of signal level; thus, the dc offset itself remains zero, independent of level over a wide range. It will be noted that  $R_s$  cannot be adjusted to

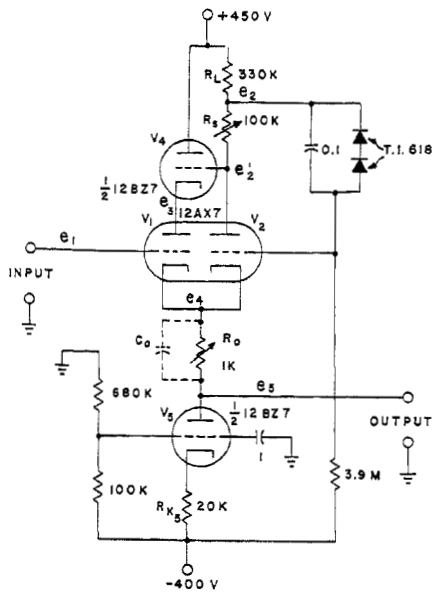


Fig. 9—The acf-3 circuit.

make both  $G_4$  and  $G_5$  simultaneously unity, because of the ac drop across  $R_0$ . Since  $R_0$  is so much smaller than the differential resistance of  $V_5$ , this drop will be exceedingly small, however, and can be even further reduced if necessary by means of the large capacitor  $C_0$ .

For most applications, it will be best to make  $G_5 = 1$

and rely on the fact that  $G_4$  will then be exceedingly close to unity so that the grid-cathode bias of  $V_1$  will still remain nearly constant keeping the dc offset very nearly independent of level. Note that when dc offset is of no consequence,  $R_0$  may be omitted. Finally, it is worth mentioning that for both the acf-2 and the acf-3, the resistances  $R_L$ ,  $R_s$ , and  $R_{K_5}$  can all be adjusted to values which will make the output level zero whether the input grid is floating or grounded. Under these conditions, this grid will float at ground potential, there will be no input-output dc offset, and the zero offset will be independent of source resistance.

## BIBLIOGRAPHY

- [1] Macdonald, J. R. "Active-Error Feedback and Its Application To A Specific Driver Circuit," PROCEEDINGS OF THE IRE, Vol. 43 (July, 1955), pp. 808-813.
- [2] Macdonald, F. R. "A Multi-Loop Self-Balancing Power Amplifier," IRE TRANSACTIONS, Vol. AU-3 (July-August, 1955), pp. 92-107.
- [3] Valley, G. E., Jr. and Wallman H. *Vacuum Tube Amplifiers*. (Massachusetts Institute of Technology, Radiation Laboratory Series, Vol. 18.) New York: McGraw-Hill Book Company, Inc., 1948, pp. 442-443.
- [4] Sallen, R. P. and Key, E. L. "A Practical Method of Designing RC Active Filters," IRE TRANSACTIONS, Vol. CT-2 (March, 1955), pp. 74-85.
- [5] Margolis, S. G. "On the Design of Active Filters With Butterworth Characteristics," IRE TRANSACTIONS, Vol. Ct-3 (September, 1956), p. 202.
- [6] Macdonald, J. R. Paper in preparation.
- [7] Macdonald, J. R. "An AC Cathode Follower Circuit of Very High Input Impedance," *Review of Scientific Instrumentation*, Vol. 25 (February, 1954), pp. 144-147.

